ORGANIC PROCESS RESEARCH & DEVELOPMENT
OPR&D

pubs.acs.org/OPRD Article

Streamlined Synthesis of a Bicyclic Amine Moiety Using an Enzymatic Amidation and Identification of a Novel Solid Form

Maria S. Brown, Michaella A. Caporello, Adam E. Goetz,* Amber M. Johnson, Kris N. Jones, Kevin M. Knopf, Samir A. Kulkarni, Taegyo Lee,* Bryan Li, Cuong V. Lu, Javier Magano, Angela L. A. Puchlopek-Dermenci, Giselle P. Reyes, Sally Gut Ruggeri, Lulin Wei, Gerald A. Weisenburger, Richard A. Wisdom, and Mengtan Zhang

Cite This: *Org. Process Res. Dev.* 2021, 25, 1419−1430 Read Online

ACCESS | Metrics & More | Article Recommendations | Supporting Information

ABSTRACT: We describe a series of improvements to the synthesis of a 3,8-diazabicyclo[3.2.1]octane derivative that result in a reduced step count and higher overall efficiency compared to previously published syntheses. Our method includes optimization and mechanistic understanding of a key diastereoselective cyclization to achieve a >95:5 diastereomeric ratio, as well as demonstration of a unique enzyme-catalyzed amidation reaction using hexamethyldisilazane as both an ammonia source and scavenger. Finally, we identify a novel cocrystal solid form of the target compound that provides improved purity and material properties. Demonstration of the new chemistry to prepare >100 kg of the target compound serves to illustrate the robustness of the new process.

KEYWORDS: *heterocyclic amine, enzymatic amidation, cocrystal, pyrrolidine, hexamethyldisilazane, bicyclic amine*

INTRODUCTION

Pharmaceutical chemistry is well-known to rely heavily on heterocyclic aromatic building blocks to construct target molecules. More recently, heterocyclic fragments that contain more sp^3 content are becoming increasingly popular. These fully or partially saturated analogues often have better solubility than aromatic counterparts and offer an increased ability to achieve critical interactions with targeted biological receptors due to their 3D shape.[1] As a result, the development of efficient syntheses of these "sp^3-rich" heterocyclic fragments is growing in relevance.

We were faced with the need to prepare large quantities of a building block containing the 3,8-diazabicyclo[3.2.1]octane system (**3**) to support a program with ongoing clinical trials.[2] Although multiple strategies exist for preparing this ring system,[3] the most commonly utilized precursor is *meso*-diethyl-2,5-dibromohexanedioate (**1**).[4] In addition to the 3,8-diazabicyclo[3.2.1]octane system, dibromide **1** has been demonstrated as a precursor to a variety of unique ring systems (Scheme 1, **1**→**2**, **1**→**4**).[5] The dibromide is produced via nonstereoselective bromination of adipic acid,[6] but the desired *meso*-diastereomer (**1**) can be selectively crystallized with a >95% diastereomeric ratio (d.r.) leaving a racemic mixture of (*R*,*R*) and (*S*,*S*) enantiomers in the mother liquor.[7,4c]

For our specific needs, we targeted the 8-benzyl derivative of the diazabicyclo[3.2.1]octane ring system (**3**, R_1 = Bn, R_2 = H). Published syntheses of benzylated analogue **3** exist in the literature,[8] and we utilized a modified version of these published routes to access the desired bicyclic amine, which was isolated as the bis-HCl salt (Scheme 2, top route). Reaction of dibromide **1** with benzylamine resulted in formation of the pyrrolidine ring via double S_N2 displacement followed by saponification/acidification to give di-acid **5**. Unfortunately, previous reports show that even when dibromide containing ≥98% of the *meso*-diastereomer is employed, the product d.r. is typically only ∼70−85% of the desired *syn*-diastereomer, which was consistent with our observations. This epimerization represents a loss in yield

Scheme 1. Several Examples of Cyclic Motifs That Can Be Accessed from *meso*-Dibromide 1

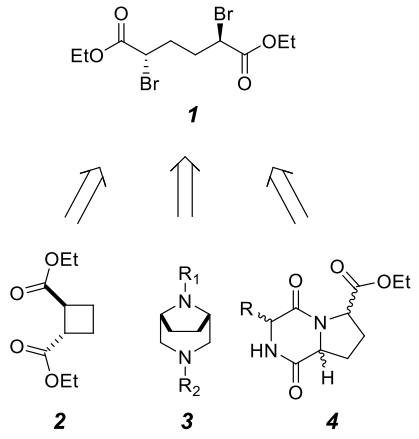

Received: April 6, 2021
Published: May 27, 2021

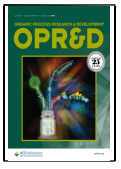

https://doi.org/10.1021/acs.oprd.1c00120
Org. Process Res. Dev. 2021, 25, 1419−1430

Scheme 2. Original Large-Scale Synthesis of Bis-HCl Salt 8 and a Proposed Alternative Route

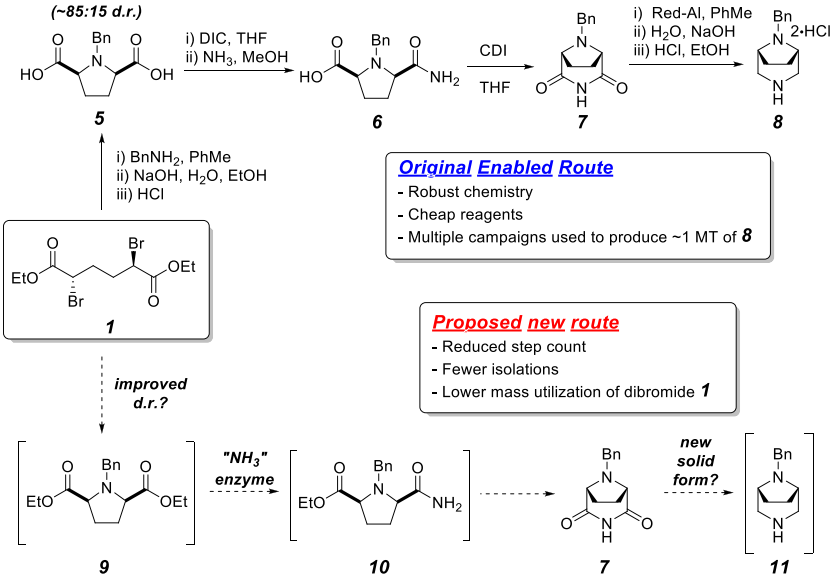

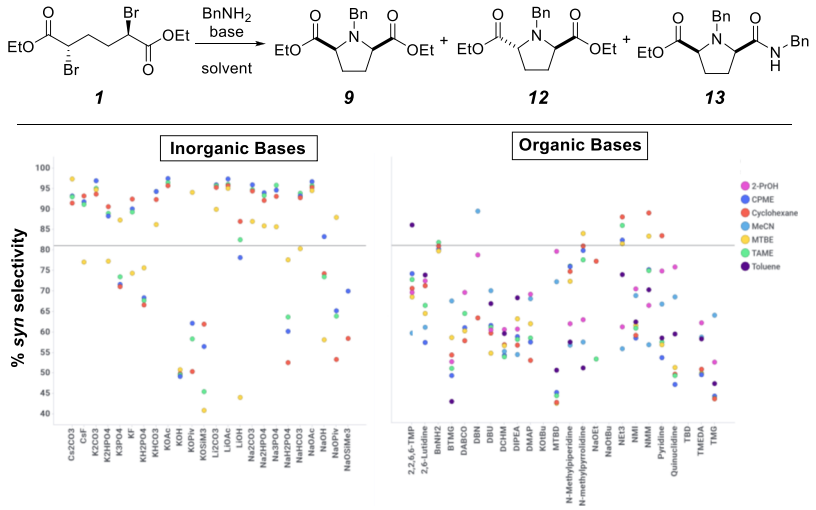

Figure 1. Influence of various bases and solvents for the conversion of dibromide **1** to *syn*-diester **9** using either inorganic bases (left) or organic bases (right). The results from inorganic base screening show only reactions performed using an aqueous solution of the bases. The performance of the original conditions (excess $BnNH_2$ as both a nucleophile and a base) is indicated by a horizontal line.

since the *syn* geometry is required to ultimately form the bicyclic scaffold. Nevertheless, conversion of *syn*-di-acid **5** to imide **7** was accomplished using a straightforward albeit somewhat lengthy sequence involving cyclic anhydride formation using diisopropylcarbodiimide (DIC), ring opening with methanolic ammonia to give amide **6**, and formation of imide **7** using 1,1′-carbonyldiimidazole (CDI). Reduction of imide **7** using sodium bis(2-methoxyethoxy)aluminum hydride (Red-Al) gave the desired amine as a freebase, which was isolated as the corresponding bis-HCl salt **8**. During our initial large-scale campaign, **8** was prepared in seven steps with an ~30% overall yield.

While subsequent campaigns resulted in slight enhancements, we believed that we could streamline this route by targeting three key areas for further development (Scheme 2, bottom route). We sought to improve the modest diastereoselectivity during formation of **9** to maximize yield as well as reduce the overall step count via a direct conversion of bis-ester **9** to amide **10**. Finally, though the bis-HCl salt was an attractive solid form due to its simplicity, it possessed several distinct disadvantages that we wanted to address by exploring alternative solid forms. This manuscript describes these improvements to the process as well as an initial multikilogram-scale demonstration of the new chemistry.

RESULTS AND DISCUSSION

Improving Diastereoselectivity in the Cyclization of 1. As mentioned above, the cyclization of *meso*-diastereomer **1** with various amines affords primarily the *syn*-diastereomer of the pyrrolidine diester, however, with a decrease in the stereochemical purity relative to the starting dibromide. During early campaigns, we utilized an excess of benzylamine (to serve as both the nucleophile and base) in toluene, which gave an ~85:15 mixture of *syn:anti* diastereomers despite starting with **1** that was ≥98% of the *meso*-diastereomer. We found that the final diastereomeric ratio did not further change with prolonged reaction times, and subjecting purified *syn* isomer **1** to the reaction conditions did not result in any stereo-

https://doi.org/10.1021/acs.oprd.1c00120
Org. Process Res. Dev. 2021, 25, 1419−1430

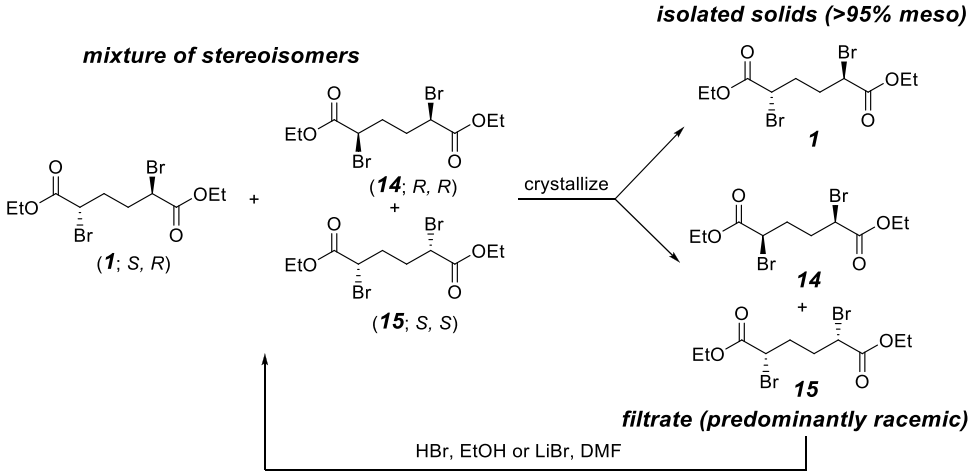

Figure 2. Epimerization of bromide stereoisomers as reported in refs 5d and 13.

chemical scrambling. Epimerization of pyrrolidine diester derivatives such as **9** has been demonstrated using stronger metal-alkoxide bases that results in a near 1:1 ratio of the two diastereomers.[9] This is also in line with quantum mechanical calculations that suggest that the two diastereomers are very similar in energy.[10] However, since we did not observe any measurable amount of epimerization of diester **9** using bases such as benzylamine, triethylamine, or even DBU, we reasoned that epimerization occurred prior to formation of the carbon−nitrogen bonds and that we could potentially suppress this by changing the reaction conditions.

We embarked on screening various solvents and bases to explore the impact on the diastereomeric ratio during formation of ester **9**. We found that nonpolar solvents (toluene, MTBE, and cyclohexane) tended to give higher diastereoselectivity than polar solvents (MeCN and 2-PrOH) and that inorganic bases gave superior selectivity compared to organic bases. A portion of the screening data is shown in Figure 1, which highlights the significantly higher selectivity for **9** when using inorganic bases vs organic bases. More detailed screening data is available in the Supporting Information. Of the >20 organic bases evaluated under various conditions, the selectivity rarely exceeded the ∼85:15 ratio previously seen. In contrast, many of the inorganic bases screened showed a >95:5 preference for the *syn* diastereomer. These inorganic bases were screened using "anhydrous" conditions that gave a heterogeneous reaction mixture, as well as conditions where the inorganic base was dissolved in water, which resulted in a biphasic mixture with the organic solvents. On vial scale, similar results were seen between these two modes, but during larger-scale experiments, the "anhydrous" conditions showed more variability in terms of selectivity and reaction rates, so we elected to proceed with the biphasic solvent mixture.[11] The use of inorganic bases under biphasic conditions (K_2CO_3 in toluene/water) for cyclization of dibromide **1** has been previously reported; however, in these cases, the reported selectivity is only 75−80% *syn*, which is significantly lower than what we observed under our optimized conditions (*vide infra*).[5c12] In addition to diastereomers **9** and **12**, amide **13** was formed in small amounts (typically <5%) under many of the conditions screened. We were pleased to see that despite the presence of aqueous basic conditions, saponification of the diesters to the corresponding acid was not a significant problem under these conditions.

During our attempts to understand the origin of the higher diastereoselectivity with inorganic bases, we relied on a key observation from published accounts focused on improving the isolated yield of *meso*-dibromide **1** during crystallization. It has been previously demonstrated that the dibromide stereoisomers can be epimerized via S_N2 displacement by bromide anions (Br^-), which can allow for recycling of the more soluble racemic isomers to increase the recovery of the more highly crystalline *meso*-diastereomer (Figure 2).[13]

We have also observed that the same epimerization as described above occurs during the reaction of dibromide **1** with benzylamine. By monitoring the diastereomeric purity of the unreacted dibromide **1** (>95% *meso* at $t = 0$) as well as the pyrrolidine diester **9** being formed during the reaction, we found that stereochemical purity continually decreases throughout the reaction. Especially in the case of the dibromide, this erosion in the *meso* content occurs to a much greater extent than could be expected solely from reaction rate differences between the different isomers (Figure 3, solid orange line). The extent of erosion seen in the remaining dibromide **1** was less when the biphasic conditions with an inorganic base were utilized (Figure 3, dashed orange line). The lower selectivity during cyclization is therefore a result of epimerization of *meso*-dibromide **1** caused by the bromide anion byproduct. This results in an increasingly unselective formation of esters **9** and **12** as the reaction progresses. We hypothesize that the use of biphasic conditions helps sequester the bromide anion in the aqueous layer (as the alkali salt) due to the low solubility of bromide salts in the nonpolar organic solvents.[14] Consistent with this hypothesis, we have observed that spiking in a more organic-soluble bromide anion such as tetrabutylammonium bromide (TBAB) into the biphasic conditions results in lower diastereoselectivity.

Despite the higher levels of selectivity seen using inorganic bases, we found that many of the reactions were quite slow, often taking ≥48 h to achieve full conversion. While some reactions in 2-MeTHF were found to proceed with higher selectivity in ∼24 h, the cost of this solvent relative to other options from the initial screening (toluene, MTBE, and cyclohexane) as well as the deleterious impact that it had on the downstream enzymatic transformation prompted us to pursue further optimization with alternative solvents. We therefore performed a second round of screening that focused

https://doi.org/10.1021/acs.oprd.1c00120
Org. Process Res. Dev. 2021, 25, 1419−1430

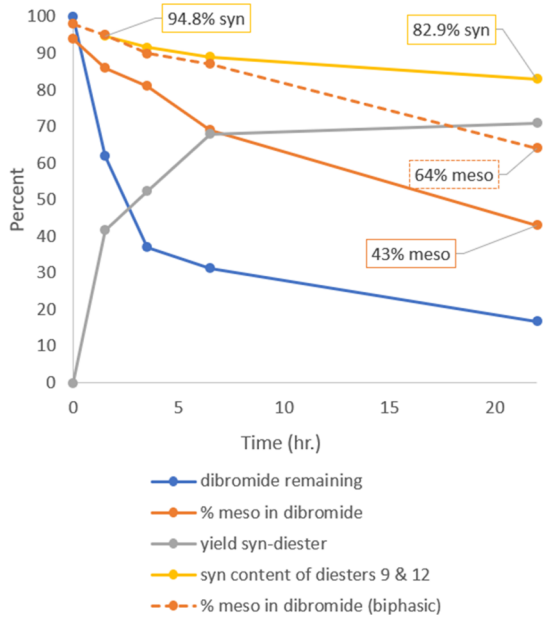

Figure 3. Monitoring the chiral purity of *syn*-diester **9** and unreacted dibromide isomers during pyrrolidine formation. The solid lines are from a reaction using the original conditions of excess $BnNH_2$ in toluene. The *meso*-dibromide is seen to epimerize significantly over the course of the reaction (orange solid line) resulting in the selectivity for *syn*-product formation decreasing throughout the reaction (yellow solid line). When using aqueous $NaHCO_3$/2-MeTHF (orange dotted line), the *meso*-dibromide undergoes significantly less epimerization over the course of the reaction.

on identifying solvent/base pairs that could maintain the high diastereoselectivity while reducing the overall reaction time (Table 1).[9] Ultimately, we identified the use of aqueous trisodium phosphate (Na_3PO_4) as the preferred base, using toluene as the organic phase, which also allowed for a higher reaction temperature than MTBE. By reducing the overall volumes of the reaction, we could further accelerate the reaction to give an ~90% assay yield of **9** (97:3 *syn*:*anti*) with a typical reaction time of 24−28 h. Following the reaction, an aqueous citric acid wash is performed to remove any residual benzylamine while minimizing the losses of pyrrolidine **9**.

Table 1. Impact of Reaction Conditions on the Rate of Ester 9 Formation

base[a]	solvent	temp./time[b]	ester (**9**) (% area)
$NaHCO_3$	2-MeTHF (5 V) H_2O (5 V)	75 °C/24 h	84
K_2CO_3	MTBE (2.5 V) H_2O (2.5 V)	55 °C/24 h	76
K_2CO_3	MTBE (5 V) H_2O (5 V)	55 °C/120 h	85
K_3PO_4	MTBE (5 V) H_2O (5 V)	55 °C/78 h	87
K_3PO_4	PhMe (5 V) H_2O (5 V)	75 °C/48 h	94
Na_3PO_4	PhMe (5 V) H_2O (5 V)	75 °C/48 h	95
Na_3PO_4	PhMe (2.5 V) H_2O (5 V)	75 °C/24 h	92

[a]Reactions were run using 3.0 equiv of the base. [b]Reactions were monitored by UPLC until >97% conversion was achieved.

Enzymatic Amidation of Ester 9. Despite the simplicity of the original four-step sequence used to convert bis-ester **9** to imide **7**, we speculated that we could reduce the overall step count by targeting primary amide **10** as a precursor to the desired imide. For this transformation, we explored the feasibility of an enzymatic amidation to form the amide selectively.[15] Specifically, we were pleased to find that different preparations of immobilized *Candida antarctica* lipase B (CalB) showed the most promising for this transformation[16] using either solutions of ammonia in alcoholic solvents or ammonium carbamate with MTBE as the organic solvent at 40−50 °C (Figure 4).[17] Unfortunately, all attempts to utilize

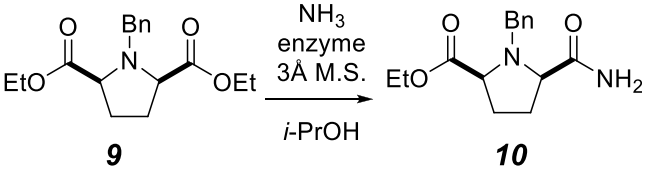

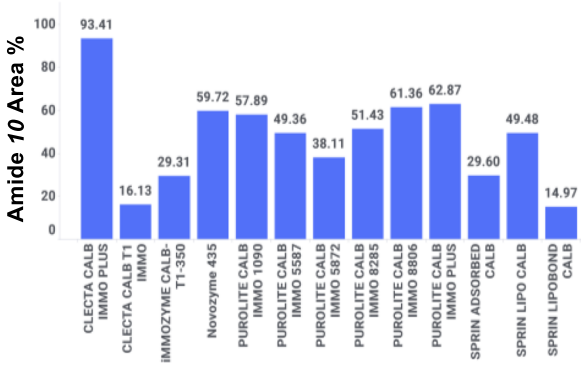

Figure 4. Initial screening of amidation using various immobilized CalB sources. Conditions: 2.5 mg of ester **9**, 25 mg of an enzyme, 25 mg of 3 Å M.S., 2 M ammonia in *i*-PrOH (0.5 mL), 50 °C, and 22 h.

liquid enzyme preparations showed essentially no conversion during this initial evaluation, highlighting the importance of the solid support for stabilizing the enzyme under the reaction conditions. After the initial screenings, further optimization was performed with several of the top enzyme candidates to understand differences in performance. We ultimately selected CalB Immo Plus from Purolite as the preferred option due to a good balance of activity and cost.

Unfortunately, both ammonia sources from the initial screening work had aspects that made them unattractive. The presence of ethanol is deleterious to enzyme activity, requiring the use of ammonia solutions in either methanol or isopropanol. Unfortunately, with both solvents, we observed varying amounts of transesterification byproducts.[18] For ammonium carbamate, the continual release of CO_2 was unattractive as well as the large amount of solids that were present in the reaction. Molecular sieves (or $CaCl_2$) were also required in both cases to minimize carboxylic acid byproducts that formed from the small amount of water introduced with the ammonia sources as well as to adsorb the EtOH byproduct that is generated from the desired transformation and prevent enzyme poisoning.

To address these drawbacks, we explored the use of hexamethyldisilazane (HMDS) as an alternative ammonia

https://doi.org/10.1021/acs.oprd.1c00120
Org. Process Res. Dev. 2021, 25, 1419−1430

source. We hypothesized that reaction with any water or alcohol present in the reaction mixture would gradually liberate ammonia while also having the benefit of removing these problematic species by converting them to (presumably inert) silylated species (Scheme 3, **16**→**17** and **16**→**18**).[19] To our

Scheme 3. Reaction of HMDS with Various Protic Species Present during the Enzymatic Amidation

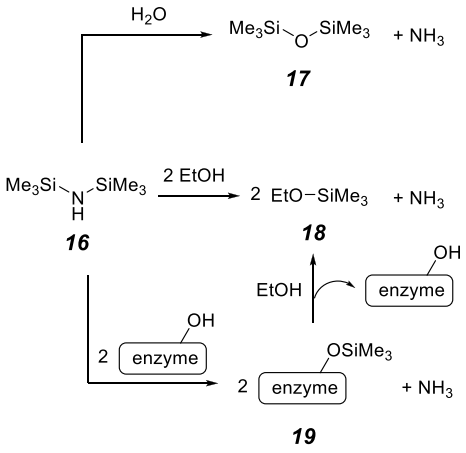

knowledge, the use of HMDS has not been demonstrated previously in enzymatic transformations, but we were delighted to find that it gave the desired amide product in good yield. Initially, the high enzyme load that was required for good activity (~1 g immobilized enzyme/g substrate) prompted us to explore the possibility of recycling the enzyme through multiple runs. We observed that at the end of the reaction, the enzyme showed significantly decreased activity, and we speculated that HMDS could be reacting with various sites on the enzyme leading to diminished activity (Scheme 3, **16**→**19**). Indeed, we found that soaking the enzyme beads in MTBE containing a stoichiometric amount of EtOH (relative to HMDS charged) regenerated the activity. Further exploration of this enzyme washing protocol suggested that the specific conditions employed had some impact on the subsequent run (see the Supporting Information); however, we were able to successfully demonstrate that the same sample of an enzyme could be reused for at least 8 cycles with minor impact to the overall reaction profile as shown in Figure 5. Furthermore, the fact that there is no continual decline in enzyme performance over sequential runs (e.g., cycle 5 outperforms cycle 2) is consistent with our belief that the enzyme deactivation by HMDS is largely reversible (**16**→**19**→**18**, Scheme 3) and that the washing protocol is critical to restoring enzyme performance.

Ultimately, we sought to reduce the overall enzyme loading, and through these efforts, we discovered that the presence of small amounts of water had a dramatic impact on reaction performance. We were excited to find that addition of a substoichiometric amount of water (typically 0.5−0.8 equiv) allowed for a 6−8-fold reduction in the immobilized enzyme from 1 to 0.12−0.15 g/g while maintaining good performance. In the case of immobilized enzymes, the actual mass of the enzyme is quite low, with the bulk of the mass coming from the solid support. For CalB Immo Plus, the protein loading is reported to be approximately 24 mg/g_{wet}, which corresponds to an enzyme loading of 0.3−0.4% (w/w) relative to diester **9**.[20] The exact role of water in this transformation is not

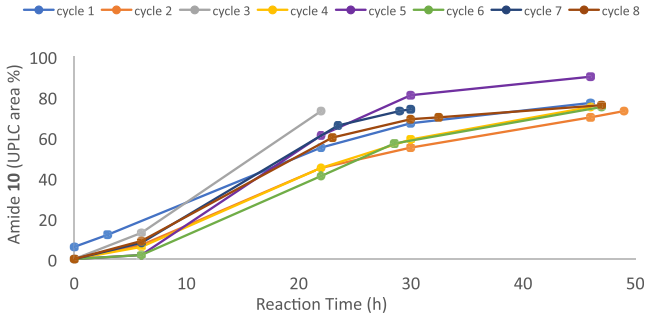

Figure 5. Recycling of a single batch of enzymes during conversion of **9** to amide **10**. Conditions: 2.0 g of ester **9**, 1 g/g CalB Immo Plus, 40 mL of MTBE, 1.5 equiv of HMDS, and 40 °C. Following the reaction, the enzyme was washed with MTBE then soaked with EtOH in MTBE (~1 equiv of EtOH) for several hours before a final MTBE wash. See the Supporting Information for full details on the washing protocol used after each run.

completely understood although numerous experiments show that it provided a consistent and reproducible benefit. We hypothesize that a critical amount of water is needed to maintain a hydration sphere around the enzyme for optimal performance.[21] Indeed, with too little water, enzymatic activity drops dramatically (and the appearance of silylated analogues of **10** is sometimes seen), but with too much water, the undesired carboxylic acid byproduct is formed preferentially, which does not undergo conversion to the desired amide.[22] We have observed that maintaining the solution water content around 0.02−0.1% (as measured by coulometric KF titration) gives good performance although this most likely does not represent the true water content[23] since a portion of the water is adsorbed onto the enzyme and not detected by solution measurements.[24] After significant optimization, we settled on a charging strategy where ~1.3 equiv of HMDS and ~0.5−0.6 equiv of water were utilized. At the start of the reaction, approximately half of each reagent was charged, and then, the remaining amount was charged in periodic doses to achieve full conversion. Reactions were typically complete within 48−72 h and showed >90% (a/a) amide **10**, with <5% (a/a) of carboxylic acid byproduct.[25]

We had originally hoped to perform the pyrrolidine formation, enzymatic amidation, and imide formation (**9**→**10**→**7**) without isolation to help streamline the overall process. While it was possible to telescope the solution of pyrrolidine **9** into the enzymatic reaction, we did observe variability across different ingoing batches of **9** with some reactions stalling out before achieving full conversion. We performed numerous spiking studies to understand the tolerability of different impurities/byproducts that were plausible in ester **9** as well as studies to identify suitable washes or treatments that might provide a consistent material for the enzymatic reaction. Ultimately, we opted to isolate the HCl salt of bis-ester **9** and then perform a salt-break prior to the enzymatic step, which helped normalize the performance of the ingoing material. Fortunately, we were able to telescope amide **10** into the imide formation after a simple filtration to remove the enzyme.

Attempts to cyclize amide **10** by heating in refluxing toluene showed no conversion to the desired imide. Indeed, previous reports demonstrate that ring closure of amides similar to **10** can be accomplished thermally although temperatures in excess of 200 °C are required.[4e,26] Alternatively, we opted to treat crude amide **10** with a solution of potassium *tert*-butoxide

https://doi.org/10.1021/acs.oprd.1c00120
Org. Process Res. Dev. 2021, 25, 1419−1430

(KO*t*Bu) in THF to effect rapid ring closure at room temperature and intercept imide **7**, which served as the penultimate intermediate in our initial synthetic route. Numerous examples of imide reduction on substrates similar to **7** have also been reported, typically using $LiAlH_4$ to produce the bicyclic diamine. However, during work on our initial route, we identified sodium bis(2-methoxyethoxy)aluminum hydride (Red-Al) as an attractive alternative based on ease of handling as well as the convenience of using a concentrated toluene solution, which simplified the workup and allowed for direct extraction of the desired freebase amine **11** into toluene after the reduction.

Identification of a Novel Cocrystal of 11. The desired bicyclic amine **11** is a low melting solid with a melting point of 30−35 °C and is therefore more easily handled as a salt.[27] While the bis-HCl salt **8** is an obvious choice, we observed that this material tends to have low bulk density (typically 0.25−0.30 g/cm^3), poor flowability, variable levels of certain impurities and in a few cases caused minor corrosion to steel containers used for storage due to excess HCl. As a result, we explored other solid forms that might address some of these drawbacks. Rather than limiting ourselves only to various acid salts, we also explored the possibility of forming a cocrystal given the propensity of certain amines to form these ordered structures by serving as hydrogen bond acceptors.[28] It was also hoped that by employing a cocrystal, we could avoid performing a salt-break prior to using the amine in downstream reactions.

We utilized a combination of computational and experimental screening by first ranking a library of potential coformers based on their calculated ability to form strong hydrogen bonds with the desired amine **11** using commercially available COSMOquick software (Table 2, see the Supporting Information for full results). For each potential coformer, the software calculates the mixing enthalpy (H_{mix}), which corresponds to the enthalpy difference between a supercooled mixture of the two components and the enthalpies of the two individual components.[29] This enthalpy value relates to the tendency of the two species to cocrystallize. Application of a correction to H_{mix} based on the number of rotatable bonds in the two molecules gives the "f_fit" parameter, which tends to give better predictive power.[30]

Table 2. Top Computational Hits for Potential Coformers for Amine 11 Using COSMOquick

coformer	coformer ranking	H_{mix} (kcal/mol)	f_fit
phenol	1	−3.64	−2.11
4,4-biphenol (**20**)	2	−4.33	−1.78
saccharin	3	−1.47	0.06
p-hydroxybenzamide	4	−1.76	0.79
butyl acetate	5	−2.70	0.87
fucose	6	−2.12	0.94
thiabendazole	7	−0.48	1.05
α-D-ribopyranose	8	−1.88	1.18
imidazole	9	−0.32	1.21
2-aminopyrimidine	10	−0.21	1.32

The top computational hits were then evaluated experimentally to determine whether mixing of amine **11** with each coformer resulted in a new solid form, as determined by PXRD analysis. Several new cocrystals were identified, and we ultimately selected 4,4′-dihydroxybiphenyl (**20**, CAS no. 92-88-6) as the most attractive candidate. 4,4′-Dihydroxybiphenyl[31] is produced on a >1000 MT/year scale, is used widely as a key building block in the liquid crystal[32] and high-performance polymer[33] fields, and with a cost of ∼$30/kg contributes little to the economics of the overall process. We were further pleased to find that when this coformer was mixed with amine **11**, it resulted in a crystalline material that was composed of a 2:1 ratio of amine **11** to biphenol **20** (Figure 6). A benefit of

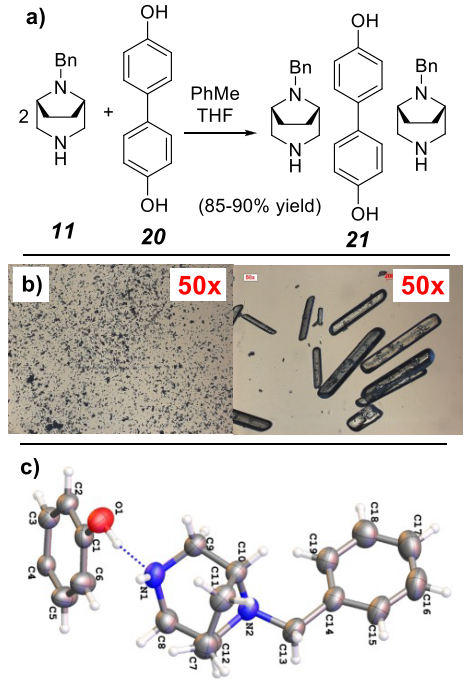

Figure 6. (a) Formation of cocrystal **21**. (b) Microscopy comparison of bis-HCl salt **8** (left) with cocrystal **21** (right). (c) X-ray crystal structure of **21** showing the unit cell with key hydrogen bonding interaction between O1 and N1 (distance is 1.73 Å).

this 2:1 complexation is that the active potency of amine **11** is only slightly lower than the original bis-HCl salt (68.5% for the cocrystal vs 73.5% for the bis-HCl salt). Furthermore, the cocrystal formed well-behaved crystalline particles (typical bulk density of 0.5−0.6 g/cm^3), had much better flowability, is nonhygroscopic, and to date has given only a single polymorph across various conditions.

Further optimization of the crystallization procedure ultimately produced a cocrystal in an 85−90% yield based on the assay concentration of amine **11** present. Following reduction of imide **7** and aqueous workup, a solution of amine **11** in toluene was obtained. This turned out to be an optimal solvent for isolation of the desired cocrystal due to the low solubility of this species in toluene.[34] The biphenol also has poor solubility in toluene, but it can be readily dissolved to give a ∼20% (w/w) solution in THF. We found that adding 0.55−0.60 equiv of biphenol (as a THF solution) to a heated toluene solution of amine **11** followed by gradual cooling resulted in recovery of the desired cocrystal (Figure 6a). The addition of the biphenol as a THF solution as opposed to as a solid charge minimizes the risk of the final solids containing free 4,4′-biphenol due to the relatively low solubility of this coformer.

Crystallization of **21** was also found to provide a significant purity upgrade. Although prior batches of the bis-HCl salt **8** showed generally high purity (>98% by HPLC), various low-

https://doi.org/10.1021/acs.oprd.1c00120
Org. Process Res. Dev. 2021, 25, 1419−1430

level impurities were observed across different batches of this material (Figure 7). When isolating cocrystal **21**, we

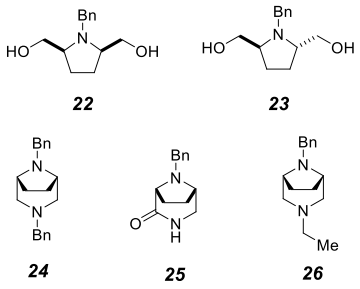

Figure 7. Impurities observed in amine **11** used for spiking studies.

consistently observed HPLC purities of >99.8% (a/a). Even when numerous impurities (**22**–**26**, Figure 7) were intentionally introduced to provide a solution of amine **11** with an ingoing purity of ∼90% by HPLC, the final cocrystal was still isolated with >99.9% HPLC purity.[9]

In addition to providing a robust purification point for the desired amine, cocrystal **21** can also serve as a useful precursor, analogous to the bis-HCl salt (Scheme 4). Cocrystal **21** can be easily broken using a single partition between aqueous potassium hydroxide (KOH) solution and an organic solvent such as MTBE, toluene, 2-MeTHF, or DCM. In all cases, >98% of the ingoing amine **11** was recovered in the organic layer, whereas the undesired 4,4′-dihydroxybiphenyl was extracted into the aqueous layer as the bis-potassium salt. In some cases, cocrystal **21** can also be used directly (without complication from the biphenol) due to the higher nucleophilicity of the amine fragment. Both amidation using carboxylic acid **27** with propylphosphonic anhydride (T3P) and S_NAr reaction with pyrrolopyrimidine **29** proceeded smoothly to give the respective products **28** and **30** resulting from a reaction with the amine. Following each reaction, the unreacted biphenol was readily removed via extraction with aqueous KOH before isolation of the desired product.

Scheme 4. Synthetic Utility of Cocrystal 21

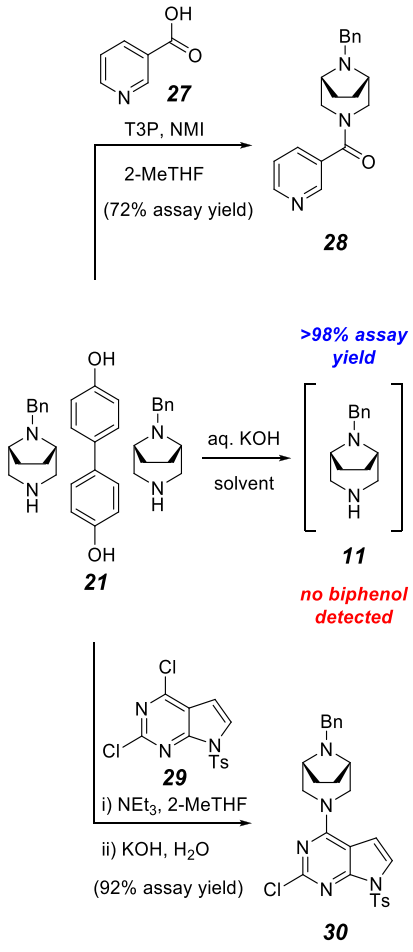

Kilogram-Scale Manufacturing of 21. Having identified a number of improvements to the overall process for producing amine **11**, we successfully demonstrated this technology on multi-kilogram scale, as shown in Scheme 5. During the formation of bis-ester **9**, the biphasic conditions performed as expected based on lab trials and resulted in high selectivity for the *syn* diastereomer (>96:4 dr for both batches). Isolation as the HCl salt **31** provided a further upgrade to yield a material that had ≥99.5% purity by HPLC. During the initial batch, the isolated yield was only 70%, which was much lower than expected, and the mother liquors were found to contain an additional ∼14% yield of the product. For the second batch, the amounts of HCl and EtOH used during salt isolation were decreased, which resulted in a much improved 83% isolated yield without any change in purity.

The initial batch of the amidation reaction utilized a 15% (w/w) enzyme loading and charged HMDS and water in only two portions (t = 0 and 28 h). The reaction reached completion after 42 h; however, it was found that the level of the monoacid impurity was higher than desired (∼9% by area), which is likely due to having too much water present during the initial stages of the reaction. For the second batch, the enzyme loading was decreased to 12.5% (w/w), and the charging strategy was adjusted to utilize less water upfront followed by an increased number of smaller charges during later portions of the reaction. This had the desired effect of reducing the amount of the monoacid impurity formed, although it resulted in a slower reaction that required ∼85 h to reach full conversion. The profile for this reaction is shown in Figure 8 (solid lines), along with the levels of the various silyl species that can be monitored by GC (Figure 8, dashed lines). Further optimization of the charging strategy will likely allow for shorter reaction times while still maintaining the high selectivity for the desired amidation reaction. Given the significant reduction in enzyme loading that had been achieved and the fact that only two batches using the enzymatic transformation were planned, we opted not to recycle the enzyme during this campaign. Ultimately, a further understanding of the economic impact of recycling the enzyme vs purchasing fresh supplies may be beneficial for larger campaigns or processes where the enzyme cost is a larger contributor.

Following amidation, the product solution is filtered to remove the enzyme and then concentrated before potassium *tert*-butoxide is added as a THF solution to effect ring closure and form imide **7**. After pH adjustment using aqueous citric acid and brine, the THF solution is again concentrated before water is added to promote crystallization of imide **7**. Overall, we found that this 2-step sequence produced imide **7** in an average of 81% yield from diester **9**, despite the lower yield for the initial batch due to elevated levels of the monoacid impurity.

https://doi.org/10.1021/acs.oprd.1c00120
Org. Process Res. Dev. 2021, 25, 1419−1430

Scheme 5. Pilot Plant-Scale Synthesis to Produce 110 kg of Cocrystal 21

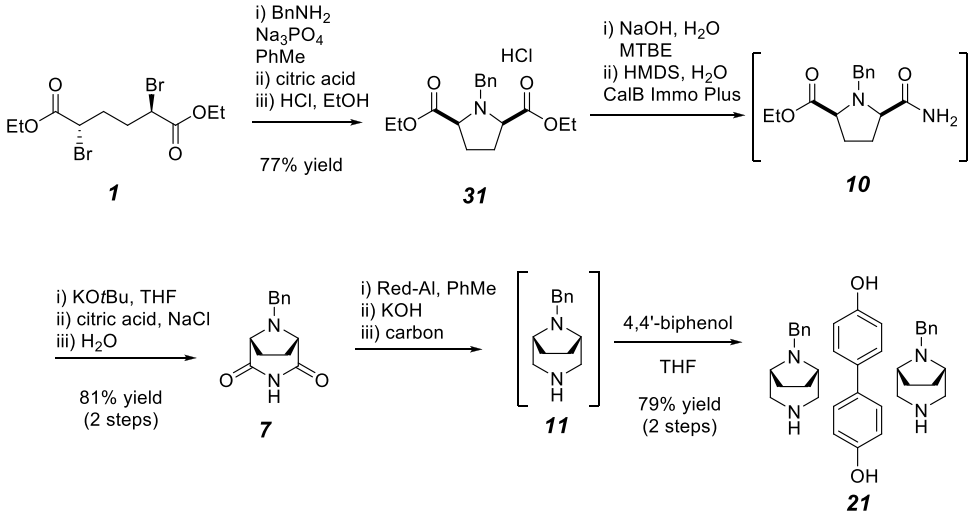

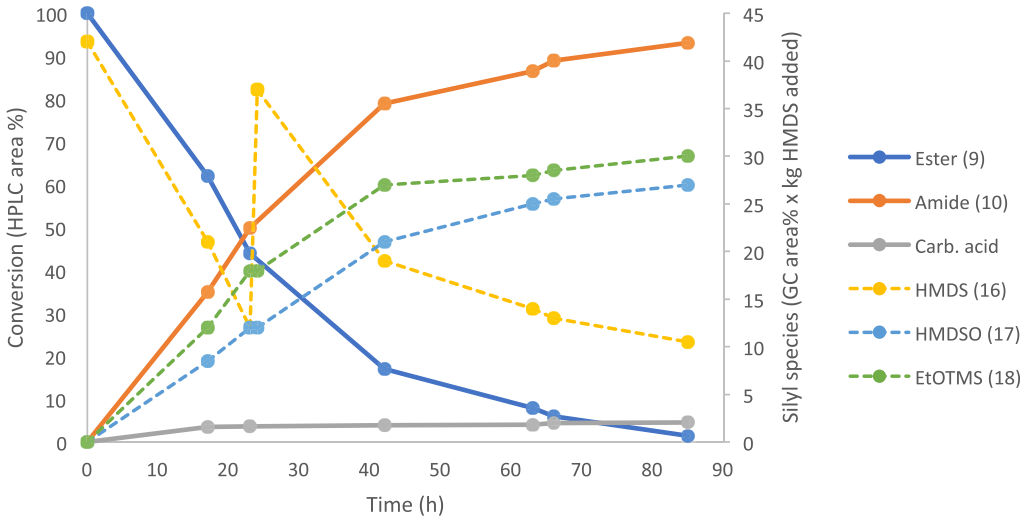

Figure 8. Reaction profile showing conversion of various pyrrolidine species by HPLC (solid lines) and separate tracking of various silyl species by GC (dashed lines).

Reduction of imide **7** was performed using a nearly identical process to earlier campaigns that targeted the bis-HCl salt. The initial reduction is facile, giving amide intermediate **25** (see Figure 7), which is then gradually heated to 65 °C to promote the subsequent reduction. After the reaction is complete, it is quenched via slow addition into a large excess of aqueous sodium hydroxide, which gives a solution of amine freebase **11** in toluene. Past experience with the bis-HCl salt had shown that the final material sometimes possessed a light brown/tan color that was difficult to remove during downstream chemistry.[35] Therefore, we opted to circulate this toluene mixture through a carbon cartridge to help improve the color. Formation of the cocrystal as described above resulted in the isolation of 110 kg of cocrystal **21**, which corresponds to a 79% yield over the reduction and cocrystal formation sequence.[36]

SUMMARY/CONCLUSIONS

In summary, we have demonstrated a streamlined process to prepare bicyclic amine **11** as well as identified a novel cocrystal that serves as a convenient solid form for isolation. In addition to improving the performance of key reactions used in the synthesis, we have identified a shorter sequence to construct the bicyclic moiety using an enzymatic amidation that employs HMDS as both the ammonia source and the reagent to help sequester byproducts that would otherwise reduce enzyme performance. We have demonstrated the robustness and scalability of this chemistry by preparing >100 kg of the target compound with high purity in similar performance to lab runs. When compared to the initial process to prepare bis-HCl salt **8**, we have decreased both the number of steps and isolated intermediates while also increasing the overall yield from 29.8 to 49.6%. This results in an ~40% reduction in the amount of the starting dibromide **1** needed to prepare the desired bicyclic amine **21**, even when accounting for potency differences of the different solid forms. Based on observations during this initial large-scale campaign, we believe that further improvement to the route presented here would offer even more benefit compared to existing technology.

EXPERIMENTAL SECTION

Preparation of Pyrrolidine 31. To a 2000 L vessel were added water (840 kg) and tribasic sodium phosphate (160 kg,

https://doi.org/10.1021/acs.oprd.1c00120
Org. Process Res. Dev. 2021, 25, 1419−1430

825 mol, and 2.12 equiv). To this cloudy suspension were added dibromide **1** (140 kg, 389 mol, and 1.00 equiv), toluene (315 kg, 2.25 g/g), and benzylamine (52 kg, 490 mol, and 1.2 equiv), and the vessel was made inert with nitrogen. The contents were heated to 75 °C and held until <1% of dibromide **1** remained (~26 h). After cooling to 40 °C, additional water (280 kg) and toluene (285 kg) were added, and the layers were separated. The organic phase was washed twice with an aqueous solution containing 10% (w/w) citric acid and 10% (w/w) NaCl (2 × 530 kg) followed by a final wash with 10% aqueous NaCl (130 kg). The solution was concentrated under vacuum to reduce the amount of toluene to ~400 kg, and then, distillation continued (with toluene replacement) until a water content of 0.03% (as measured by KF) was obtained. The reaction was cooled to 10 °C, and ethanol (6 kg) and 1,4-dioxane (85 kg) were added. Into this solution was slowly bubbled gaseous HCl (13 kg, 356.6 mol, and 0.92 equiv), and the slurry was cooled to 5 °C. The solids were filtered and washed with toluene (110 kg), and the pyrrolidine salt **31** was dried until 138.2 kg (110.6 kg corrected, 83% yield, and ~20% toluene by assay) of an easily handled solid was obtained. HPLC purity: >99.5% (a/a, excluding toluene); ^{1}H NMR (400 MHz, DMSO-d_6): δ 11.47 (br s, 1H), 7.60−7.50 (m, 2H), 7.40−7.31 (m, 3H), 4.39 (s, 2H), 4.20 (br s, 2H), 4.01 (app. qd, J = 7.2, 1.7 Hz, 4H), 2.4−2.26 (m, 2H), 2.10−1.98 (m, 2H); ^{13}C NMR (100 MHz, DMSO-d_6): δ 170.0, 133.4, 131.0, 129.2, 128.8, 66.7, 61.8, 58.7, 28.0, 14.3; HRMS (ESI/Orbitrap) m/z: $[M + H]^+$ calcd for $C_{17}H_{24}O_4N$, 306.1700; found, 306.1701. Anal. calcd for $C_{17}H_{24}ClNO_4$: C, 59.73; H, 7.08; N, 4.10. Found: C, 59.76; H, 6.78; N, 4.13.

Preparation of Imide 7. To a 2000 L vessel were added sodium phosphate (7.5 kg, 39 mol, and 0.12 equiv), water (140 kg), pyrrolidine **31** (138.2 kg, 110.56 kg corrected, 323.4 mol, and 1.000 equiv), and MTBE (260 kg).While maintaining a temperature of 10−15 °C, 33% NaOH (33.1 kg, 273.1 mol, and 0.844 equiv) was added, resulting in a solution with pH = 9.2. The layers were separated, and the organic phase was washed with a 10% sodium chloride solution (30 kg) followed by water (30 kg). The organic phase was concentrated at 40−45 °C under vacuum until ~1/2 of MTBE had been removed and then further distilled (with MTBE replacement) until a water content of 0.1% (as measured by KF) was obtained.

To this MTBE solution were added the CalB Immo Plus immobilized enzyme (12.0 kg), MTBE (540 kg), HMDS (42.00 kg, 260.2 mol, and 0.8 equiv), and water (1.50 kg, 83.3 mol, and 0.258 equiv), and the reaction was warmed to 41−43 °C. To the reaction was added additional water (1.0 kg, 0.48 kg, 0.17 kg, and 0.284 equiv total) after 24.5, 43.5, and 64 h, and additional HMDS (25.00 kg, 154.9 mol, and 0.47920 equiv) was added after 25 h. After 86 h, the reaction was filtered to remove the immobilized enzyme, which was washed with MTBE (130 kg) to give 1267 kg of an MTBE solution containing amide **10**. HPLC purity: 89−93% (a/a); ^{1}H NMR (400 MHz, $CDCl_3$): δ 7.87 (s, 1H), 7.22−7.06 (m, 5H), 5.83 (s, 1H), 3.87 (q, J = 7.0 Hz, 2H), 3.77 (d, J = 13.2 Hz, 1H), 3.67 (d, J = 13.2 Hz, 1H), 3.47−3.36 (m, 2H), 2.09−1.98 (m, 2H), 1.95−1.86 (m, 1H), 1.80−1.69 (m, 1H), 1.02 (t, J = 7.2 Hz, 3H); ^{13}C NMR (100 MHz, $CDCl_3$): δ 178.3, 175.3, 137.39, 129.4, 128.5, 127.6, 67.9, 66.4, 61.0, 59.1, 30.7, 30.5, 14.1; HRMS (ESI/Orbitrap) m/z: $[M + H]^+$ calcd for $C_{15}H_{21}O_3N_2$, 277.1547; found, 277.1548.

The MTBE solution containing **10** was concentrated at 55−60 °C to remove ~1000 kg of the solvent. THF (862 kg) was added, and the mixture was cooled to 15 °C. To this solution was added potassium *tert*-butoxide (20% in THF, 180 kg, 321 mol, and 0.992 equiv) over 3.5 h. After stirring for another 40 min, the reaction was cooled to 10 °C and quenched via addition of an aqueous solution of 10% citric acid and 10% sodium chloride (676 kg). After allowing the layers to settle, the aqueous layer was discarded. The organic layer was concentrated to remove ~1050 kg of the solvent, and then, water (750 kg) was added at 35−40 °C over 45 min to promote crystallization. The slurry was cooled to 20 °C and filtered, and the solids were washed with water (100 kg). Imide **7** was dried under vacuum to give 61.9 kg (83% yield from pyrrolidine **31**) of the final product. HPLC purity: >99.5% (a/a); ^{1}H NMR (400 MHz, DMSO-d_6): δ 10.90 (s, 1H), 7.38−7.31 (m, 2H), 7.31−7.25 (m, 3H), 3.70 (s, 2H), 3.62−3.57 (m, 2H), 2.30−2.20 (m, 2H), 1.85−1.76 (m, 2H); ^{13}C NMR (100 MHz, DMSO-d_6): δ 174.5, 138.0, 129.0, 128.9, 127.8, 63.6, 53.1, 26.3; HRMS (ESI/Orbitrap) m/z: $[M + H]^+$ calcd for $C_{13}H_{15}O_2N_2$, 231.1128; found, 231.1130. Analytical data is consistent with previous reports.[8c]

Preparation of Cocrystal 21. To a 1000 L vessel were added imide **7** (53.9 kg, 234 mol, and 1.00 equiv) and toluene (479 kg). The contents were cooled to 5 °C, Red-Al (70% in toluene, 312 kg, 1080 mol, and 4.62 equiv) was added over ~5 h to maintain a temperature of 0−10 °C, and then, the transfer line was washed with toluene (20 kg). The reaction was heated to 63 °C over 5 h and held for an additional 2 h until imide **7** and amide **25** had been consumed. The contents were then cooled to 25 °C and transferred gradually over 2.5 h to a vessel containing sodium hydroxide (33% in water, 550 kg, 4540 mol, and 19.4 equiv) and water (175 kg) at 5 °C. The mixture was stirred for an additional 30 min, and then, the layers were separated. The aqueous layer was further extracted with toluene (100 kg), and the organic layers were combined. The combined organic layers were washed with two portions of aqueous sodium chloride (5% in water, 66 kg). The toluene solution was dried by distillation under vacuum at 50 °C until a water content of <0.1% was obtained by KF measurement, and then, toluene was added to give an ~8% (w/w) solution of amine **11** in toluene. Two identical batches produced using the above procedure were combined and circulated through a plug containing activated carbon (2.7 kg). The final solution showed an HPLC purity of 98.2% (a/a, toluene excluded).

To a vessel containing half of the toluene solution from above (517 kg, ~42.5 kg of amine **11**, 210 mol, and 1.00 equiv) held at 60−65 °C was added 4,4′-dihydroxybiphenyl (19.5% w/w in THF, 119 kg, 125 mol, and 0.595 equiv) over 2−3 h followed by THF (7 kg). The contents were cooled to 0 °C slowly, filtered, and washed with 4:1 toluene:THF (55 kg). The resulting solids were slurried with water (230 kg), filtered, washed with water (70 kg), and dried under vacuum at 45 °C. Two batches were performed using the above procedure to produce a total of 110.2 kg of cocrystal **21** (79.4% yield from imide **7**). HPLC purity: >99.9% (a/a); ^{1}H NMR (400 MHz, DMSO-d_6): δ 7.40−7.33 (m, 8H), 7.29 (t, J = 7.3 Hz, 4H), 7.21 (t, J = 7.3 Hz, 2H), 6.80 (d, J = 8.4 Hz, 4H), 3.39 (s, 4H), 2.90 (s, 4H), 2.75 (d, J = 12.0 Hz, 4H), 2.43 (dd, J = 12.0, 1.7 Hz, 4H), 1.92−1.84 (m, 4H), 1.71−1.64 (m, 4H); ^{13}C NMR (100 MHz, DMSO-d_6): δ 156.8, 140.4, 131.6, 128.9, 128.5, 127.45, 127.0, 116.1, 60.5, 57.7, 52.2, 25.4. Anal. calcd for

https://doi.org/10.1021/acs.oprd.1c00120
Org. Process Res. Dev. 2021, 25, 1419−1430

$C_{38}H_{46}N_4O_2$: C, 77.25; H, 7.85; N, 9.48. Found: C, 77.06; H, 8.01; N, 9.48.

Representative Breaking of Cocrystal 21. To a solution of KOH in water (45%, 6.0 mL, and 8.2 equiv) were added additional water (15 mL, 3 mL/g), an organic solvent (25 mL, 5 mL/g), and cocrystal **21** (5.0 g, 8.5 mmol, and 1.0 equiv). The mixture was stirred until all solids were dissolved, and the solution was transferred to a separatory funnel. In all solvents tested, the phase split was rapid and gave a clean interface. The aqueous layer was separated and discarded. The remaining organic layer was analyzed by qNMR (1,3,5-trimethoxybenzene as an internal standard) and found to contain >98% of the theoretical amount of amine **11** based on the calculated potency. An analytical sample was obtained by concentrating the organic layer to give **11** as an oil. ^{1}H NMR (400 MHz, CD_3CN): δ 7.41 (d, J = 6.9 Hz, 2H), 7.34 (t, J = 7.4 Hz, 2H), 7.26 (t, J = 7.2 Hz, 1H), 3.47 (s, 2H), 2.99 (s, 2H), 2.86 (d, J = 12.0 Hz, 2H), 2.62 (s, 1H), 2.55 (dd, J = 12.1, 1.8 Hz, 2H), 2.05−1.96 (m, 2H), 1.78−1.71 (m, 2H); ^{13}C NMR (100 MHz, CD_3CN): δ 141.3, 129.6, 129.1, 127.6, 61.3, 58.5, 52.9, 25.8; HRMS (ESI/Orbitrap) m/z: $[M + H]^+$ calcd for $C_{13}H_{19}N_2$, 203.1543; found, 203.1543.

Amide Coupling to Produce 28. To a slurry of acid **27** (2.29 g, 18.6 mmol, and 2.2 equiv), cocrystal **21** (5.0 g, 8.45 mmol, and 1.0 equiv), and *N*-methylimidazole (1.6 mL, 20 mmol, and 2.4 equiv) in acetonitrile (50 mL) was added propylphosphonic anhydride (50% w/w in acetonitrile, 12.5 mL, 17.9 mmol, and 2.1 equiv) dropwise over 5 min, during which the reaction became fully homogeneous. After 2 h, the reaction was quenched by addition of water (3.0 mL, 20 equiv) and concentrated on the rotavap to remove any volatiles. The oil was rediluted with 2-MeTHF (75 mL) and washed twice with a mixture of 6 N KOH (18 mL, 12.5 equiv) and water (15 mL). The resulting organic solution was dried over magnesium sulfate, filtered, and concentrated to give a crude oil containing **28** (4.57 g). Analysis of this oil gave a potency of 82.30% for desired amide **28**, which corresponds to a 72% yield. An analytical sample was obtained by column chromatography (CH_2Cl_2/MeOH) for characterization purposes. UPLC purity: 95.9% (a/a); ^{1}H NMR (400 MHz, DMSO-d_6): δ 8.63 (dd, J = 4.8, 1.5 Hz, 1H), 8.59 (d, J = 1.5 Hz, 1H), 7.82 (dt, J = 7.8, 1.7 Hz, 1H), 7.46 (dd, J = 7.8, 4.9 Hz, 1H), 7.38 (d, J = 7.5, 2H), 7.32 (t, J = 7.5 Hz, 2H), 7.24 (t, J = 7.2 Hz, 1H), 4.22 (d, J = 12.5, 1H), 3.50 (s, 2H), 3.41 (d, J = 12.5 Hz, 1H), 3.22 (br s, 1H), 3.17 (d, J = 12.5 Hz, 1H), 3.06 (br s, 1H), 2.97 (d, J = 12.5 Hz, 1H), 2.04 (m, 2H), 1.65−1.55 (m, 1H), 1.49−1.37 (m, 1H); ^{13}C NMR (100 MHz, DMSO-d_6): δ 168.2, 150.2, 147.5, 139.3, 134.6, 132.2, 128.4, 128.2, 126.8, 123.5, 58.2, 58.1, 55.9, 53.7, 48.0, 24.9, 24.7; HRMS (ESI/Orbitrap) m/z: $[M + H]^+$ calcd for $C_{19}H_{22}N_3O$, 308.1757; found, 308.1758.

S_NAr Reaction to Produce 30. To a slurry of pyrrolopyrimidine **29** (582 mg, 1.70 mmol, and 2.0 equiv) and cocrystal **21** (500 mg, 0.85 mmol, and 1.0 equiv) in 2-MeTHF (7.5 mL) at 40 °C was added triethylamine (250 μL, 1.79 mmol, and 2.1 equiv), and the mixture was stirred for 20 min until the starting materials had been consumed. The reaction was transferred to a separatory funnel, and it was washed with water (5.0 mL) followed by a solution of 6 N KOH (1.2 mL, 7.2 mmol, and 8.5 equiv) in water (5.0 mL). The organic layer was dried over magnesium sulfate, filtered, and concentrated to give **30** as a crude tan foam (867 mg). Analysis of the crude solids gave a potency of 91.5% for the desired product, which corresponds to a 92% yield of **30**. UPLC purity: 98.3% (a/a); ^{1}H NMR (400 MHz, $CDCl_3$): δ 8.12 (d, J = 8.5 Hz, 2H), 7.45−7.25 (m, 8H), 6.53 (d, J = 4.1 Hz, 1H), 4.20 (br s, 2H), 3.60 (s, 2H), 3.42 (d, J = 10.1 Hz, 2H), 3.33 (s, 2H), 2.43 (s, 3H), 2.11−2.00 (m, 2H), 1.70−1.62 (m, 2H); ^{13}C NMR (100 MHz, $CDCl_3$): δ 158.6, 154.7, 152.3, 145.7, 139.0, 134.6, 129.6, 128.8, 128.7, 128.4, 127.2, 121.3, 105.1, 103.4, 58.2, 56.9, 52.3, 25.5, 22.1; HRMS (ESI/Orbitrap) m/z: $[M + H]^+$ calcd for $C_{26}H_{27}ClN_5O_2S$, 508.1568; found, 508.1573.

■ ASSOCIATED CONTENT

Supporting Information

The Supporting Information is available free of charge at https://pubs.acs.org/doi/10.1021/acs.oprd.1c00120.

Spectral data for isolated compounds, solubility data for isolated solids, computational data and additional screening results for formation of **9**, cocrystal screening data, and X-ray data for cocrystal **21** (PDF)

■ AUTHOR INFORMATION

Corresponding Authors

Adam E. Goetz − *Chemical Research and Development, Pfizer Worldwide Research and Development, Groton Laboratories, Groton, Connecticut 06340, United States;* orcid.org/0000-0003-3561-6502; Email: adam.goetz@pfizer.com

Taegyo Lee − *Chemical Research and Development, Pfizer Worldwide Research and Development, Groton Laboratories, Groton, Connecticut 06340, United States;* Email: taegyo.lee@pfizer.com

Authors

Maria S. Brown − *Chemical Research and Development, Pfizer Worldwide Research and Development, Groton Laboratories, Groton, Connecticut 06340, United States*

Michaella A. Caporello − *Chemical Research and Development, Pfizer Worldwide Research and Development, Groton Laboratories, Groton, Connecticut 06340, United States;* Present Address: Snapdragon Chemistry, Inc., 300 2nd Ave., Waltham, Massachusetts 02451, United States (M.A.C.).

Amber M. Johnson − *Chemical Research and Development, Pfizer Worldwide Research and Development, Groton Laboratories, Groton, Connecticut 06340, United States*

Kris N. Jones − *Chemical Research and Development, Pfizer Worldwide Research and Development, Groton Laboratories, Groton, Connecticut 06340, United States*

Kevin M. Knopf − *Chemical Research and Development, Pfizer Worldwide Research and Development, Groton Laboratories, Groton, Connecticut 06340, United States*

Samir A. Kulkarni − *Chemical Research and Development, Pfizer Worldwide Research and Development, Groton Laboratories, Groton, Connecticut 06340, United States*

Bryan Li − *Chemical Research and Development, Pfizer Worldwide Research and Development, Groton Laboratories, Groton, Connecticut 06340, United States;* orcid.org/0000-0002-7972-9966

Cuong V. Lu − *Chemical Research and Development, Pfizer Worldwide Research and Development, Groton Laboratories, Groton, Connecticut 06340, United States*

Javier Magano − *Chemical Research and Development, Pfizer Worldwide Research and Development, Groton Laboratories,*

Groton, Connecticut 06340, United States; orcid.org/0000-0001-7151-8032

Angela L. A. Puchlopek-Dermenci − *Chemical Research and Development, Pfizer Worldwide Research and Development, Groton Laboratories, Groton, Connecticut 06340, United States*

Giselle P. Reyes − *Chemical Research and Development, Pfizer Worldwide Research and Development, Groton Laboratories, Groton, Connecticut 06340, United States*

Sally Gut Ruggeri − *Chemical Research and Development, Pfizer Worldwide Research and Development, Groton Laboratories, Groton, Connecticut 06340, United States*

Lulin Wei − *Chemical Research and Development, Pfizer Worldwide Research and Development, Groton Laboratories, Groton, Connecticut 06340, United States*

Gerald A. Weisenburger − *Chemical Research and Development, Pfizer Worldwide Research and Development, Groton Laboratories, Groton, Connecticut 06340, United States*

Richard A. Wisdom − *Euticals GmbH, 65926 Frankfurt am Main, Germany*

Mengtan Zhang − *Analytical Research and Development, Pfizer Worldwide Research and Development, Groton Laboratories, Groton, Connecticut 06340, United States*

Complete contact information is available at: https://pubs.acs.org/10.1021/acs.oprd.1c00120

Author Contributions

The manuscript was written by A.E.G. and T.L. All authors have given approval to the final version of the manuscript.

Notes

The authors declare no competing financial interest.

■ ACKNOWLEDGMENTS

We are grateful to Chris Morris for HRMS data, Hugh Clarke for assistance with elemental analysis, and Ivan Samardjiev and Brian Samas (Pfizer, Inc.) for help with X-ray crystallography. We also acknowledge Matt Weekly, Dave Place, and Jade Nelson (Pfizer, Inc.) for helpful scientific discussions.

■ REFERENCES

(1) (a) Lovering, F.; Bikker, J.; Humblet, C. Escape from Flatland: Increasing Saturation as an Approach to Improving Clinical Success. *J. Med. Chem.* **2009**, *52*, 6752−6756. (b) Lovering, F. Escape from Flatland 2: Complexity and Promiscuity. *Med. Chem. Commun.* **2012**, *4*, 515−519. (c) Stockdale, T. P.; Williams, C. M. Pharmaceuticals that Contain Polycyclic Hydrocarbon Scaffolds. *Chem. Soc. Rev.* **2015**, *44*, 7737−7763. (d) Mykhailiuk, P. K. Saturated Bioisosteres of Benzene: Where to go Next? *Org. Biomol. Chem.* **2019**, *17*, 2839−2849. (e) Hanby, A. R.; Troelsen, N. S.; Osberger, T. J.; Kidd, S. L.; Mortensen, K. T.; Spring, D. R. Fsp^3-rich and Diverse Fragments Inspired by Natural Products as a Collection to Enhance Fragment-based Drug Discovery. *Chem. Commun.* **2020**, *56*, 2280−2283. (f) Bauer, M. R.; Di Fruscia, P.; Lucas, S. C. C.; Michaelides, I. N.; Nelson, J. E.; Storer, R. I.; Whitehurst, B. C. Put a Ring on it: Application of Small Aliphatic Rings in Medicinal Chemistry. *RSC Med. Chem.* **2021**, 448.

(2) The diazabicyclo[3.2.1]octane system is a recurring motif in bioactive compounds. For selected examples, see (a) Cignarella, G.; Barlocco, D.; Tranquillini, M. E.; Volterra, A.; Brunello, N.; Racagni, G. Interaction of 3,8-diazabicyclo(3.2.1)octanes with mu and delta Opioid Receptors. *Pharmacol. Res. Commun.* **1988**, *20*, 383−394. (b) Girard, D.; Gootz, T. D.; McGuirk, P. R. Pharmacokinetic Studies of CP-74,667, a New Quinolone, in Laboratory Animals. *Antimicrob. Agents Chemother.* **1992**, *36*, 1671−1676. (c) Rothstein, D. M.; Farquhar, R. S.; Sirokman, K.; Sondergaard, K. L.; Hazlett, C.; Doye, A. A.; GWathmey, J. K.; Mullin, S.; van Duzer, J.; Murphy, C. K. Efficacy of Novel Rifamycin Derivatives against Rifamycin-Sensitive and -Resistant *Staphylococcus aureus* Isolates in Murine Models of Infection. *Antimicrob. Agents Chemother.* **2006**, *50*, 3658−3664. (d) Lemm, J. A.; Liu, M.; Gentles, R. G.; Ding, M.; Voss, S.; Pelosi, L. A.; Wang, Y.-K.; Rigat, K. L.; Mosure, K. W.; Bender, J. A.; Knipe, J. O.; Colonno, R.; Meanwell, N. A.; Kadow, J. F.; Santone, K. S.; Roberts, S. B.; Gao, M. Preclinical Characterization of BMS-791325, an Allosteric Inhibitor of Hepatitis C Virus NS5B Polymerase. *Antimicrob. Agents Chemother.* **2014**, *58*, 3485−3495. (e) Delbary-Gossart, S.; Lee, S.; Baroni, M.; Lamarche, I.; Arnone, M.; Canolle, B.; Lin, A.; Sacramento, J.; Salegio, E. A.; Castel, M.-N.; Delesque-Touchard, N.; Alam, A.; Laboudie, P.; Ferzaz, B.; Savi, P.; Herbert, J.-M.; Manley, G. T.; Ferguson, A. R.; Bresnahan, J. C.; Bono, F.; Beattie, M. S. A Novel Inhibitor of p75-neurotrophin Receptor Improves Functional Outcomes in two Models of Traumatic Brain Injury. *Brain* **2016**, *139*, 1762−1782. (f) Fensome, A.; Ambler, C. M.; Arnold, E.; Banker, M. E.; Brown, M. F.; Chrencik, J.; Clark, J. D.; Dowty, M. E.; Efremov, I. V.; Flick, A.; et al. Dual Inhibition of TYK2 and JAK1 for the Treatment of Autoimune Diseases: Discovery of ((*S*)-2,2-Difluorocyclopropyl)((1*R*,5*S*)-3-(2-((1-methyl-1*H*-pyrazol-4-yl)amino)pyrimidin-4-yl)-3,8-diazabicyclo[3.2.1]octan-8-yl)-methanone (PF-06700841). *J. Med. Chem.* **2018**, *61*, 8597−8612.

(3) Singh, R. K.; Jain, S.; Sinha, N.; Mehta, A.; Naqvi, F.; Agarwal, A. K.; Anand, N. A Simple and Efficient Synthesis of 8-methyl-3,8-diazabicyclo[3.2.1]octane (azatropane) and 3-Substituted Azatropanes therefrom using Pyroglutamic Acid. *Tetrahedron Lett.* **2007**, *48*, 545−548.

(4) (a) Cignarella, G.; Nathansohn, G. Bicyclic Homologs of Piperazine. Synthesis of 8-Methyl-3,8-diazabycyclooctanes. *J. Org. Chem.* **1961**, *26*, 1500−1504. (b) Cignarella, G.; Nathansohn, G.; Occelli, E. *J Org. Chem.* **1961**, *26*, 2747−2750. (c) Blackman, S. W.; Baltzly, R. The Synthesis of 3,8-Diazabicyclo[3.2.1]octane and Some of Its N-Substituted Derivatives. *J. Org. Chem.* **1961**, *26*, 2750−2755. (d) Schipper, E.; Boehme, W. A Novel Ring System: 3,8-Diazabicyclo[3.2.1]octane. *J. Org. Chem.* **1961**, *26*, 3599−3602. (e) Paliulis, O.; Peters, D.; Miknius, L.; Šačkus, A. *Org. Prep. Proced. Int.* **2007**, *39*, 86−90. (f) Huang, L. J.; Teng, D. W. *Chin. Chem. Lett.* **2011**, *22*, 523−526.

(5) (a) McDonald, R. N.; Reitz, R. R. Strained Ring Systems. XII. The Synthesis of Several Dimethyl Δ^1-Cycloalkene-1,2-dicarboxylates and Certain 4-Substituted Bicyclo[2.1.0]pentane-1-carboxylic acids. *J. Org. Chem.* **1972**, *37*, 2418−2423. (b) Sturm, P. A.; Henry, D. W.; Thompson, P. E.; Zeigler, J. B.; McCall, J. W. Antifilarial Agents. Diazabicyclooctanes and Diazabicycloheptanes as Bridged Analogs of Diethylcarbamazine. *J. Med. Chem.* **1974**, *17*, 481−487. (c) Butina, D.; Sondhemier, F. Syntheses of 1-Cyclopentene-1,2-dicarboxaldehyde and 1-Cyclobutene-1,2-dicarboxaldehyde. *Synthesis* **1980**, 543−545. (d) Yamamoto, Y.; Hoshino, J.; Fujimoto, Y.; Ohmoto, J.; Sawada, S. A Convenient Synthesis of Enantiomeric Pairs of 2,5-Disubstituted Pyrrolidines of C_2-Symmetry. *Synthesis* **1993**, 298−302. (e) Guenoun, F.; Zair, T.; Lamaty, F.; Pierrot, M.; Lazaro, R.; Viallefont, P. Pyrrolidinopiperazinedione as Chiral Auxiliary and its use in Asymmetric Mannich Synthesis. *Tetrahedron Lett.* **1997**, *38*, 1563−1566. (f) Yu, W.; Vibulbhan, B.; Rosenblum, S. B.; Martin, G. S.; Vellekoop, A. S.; Holst, C. L.; Coburn, C. A.; Wong, M.; Selyutin, O.; Ji, T.; Zhong, B.; Hu, B.; Chen, L.; Dwyer, M. P.; Jiang, Y.; Nair, A. G.; Tong, L.; Zeng, Q.; Agrawal, S.; Carr, D.; Rokosz, L.; Liu, R.; Curry, S.; McMonagle, P.; Ingravallo, P.; Lahser, F.; Ansante-Appiah, E.; Fells, J.; Kozlowski, J. A. Discovery of Potent Macrocyclic HCV NS5A Inhibitors. *Bioorg. Med. Chem. Lett.* **2016**, *26*, 3793−3799.

(6) Guha, P. C.; Sankaran, D. K. Muconic Acid. *Org. Synth.* **1946**, *22*, 57−1541.

(7) Willstatter, R.; Lessing, R. Ueber *N*-Methylpyyolidin-α_1-α_2-dicarbonsäure. *Chem. Ber.* **1902**, *35*, 2065−2073.

(8) (a) Cignarella, G.; Testa, E.; Pasqualucci, C. R. Thermal and Chemical Intramolecular N→N Acyl Migration in 8-Acyl-3,8-

Diazabicyclo[3.2.1]octanes. *Tetrahedron* **1963**, *19*, 143−148. (b) Barlocco, D.; Cignarella, G.; Tondi, D.; Vianello, P.; Villa, S.; Bartolini, A.; Ghelardini, C.; Galeotti, N.; Anderson, D. J.; Kuntzweiler, T. A.; Colombo, D.; Toma, L. Mono- and Disubstituted-3,8-diazabicyclo[3.2.1]octane Derivatives as Analgesics Structurally Related to Epibatidine: Synthesis, Activity, and Modeling. *J. Med. Chem.* **1998**, *41*, 674−681. (c) Liu, H.; Cheng, T.-M.; Zhang, H.-M.; Li, R.-T. Synthesis and Structure-Activity Relationship of Di-(3,8-diazabicyclo[3.2.1]octane) Diquaternary Ammonium Salts as Unique Analgesics. *Arch. Pharm.* **2003**, *336*, 510−513.

(9) (a) Lowe, G.; Ridley, D. D. Synthesis of β-Lactams by Photolytic Wolff Rearrangement. *J. Chem. Soc., Perkin Trans. 1* **1973**, 2024−2029. (b) Kemp, D. S.; Curran, T. P. Base-Catalyzed Epimerization Behavior and Unusual Reactivity of N-Substituted Derivatives of 2,5-Dicarbalkoxypyrrolidine. Preparation of a Novel Mixed Carbamic Carbonic Anhydride by a 4-(Dimethylamino)pyridine-Catalyzed Acylation. *J. Org. Chem.* **1988**, *53*, 5729−5731.

(10) See the Supporting Information for more details.

(11) We attribute these inconsistencies to the poor solubility of many inorganic bases in the solvents being utilized. As a result, differences in the surface area and surface activity of the insoluble base can translate to differences in reaction performance. On a small scale, the grinding impact of magnetic stirrers can obviate these differences, which become more apparent at a larger scale.

(12) (a) Kubyshkin, V. S.; Mikhailiuk, P. K.; Komarov, I. V. Synthesis of 7-azabicyclo[2.2.1]heptane-1,4-dicarboxylic acid, a Rigid Non-Chiral Analogue of 2-Aminoadipic Acid. *Tetrahedron Lett.* **2007**, *48*, 4061−4063. (b) Wu, G.; Wang, D.; Zhu, W.; Shen, H.; Liu, H.; Fu, L. Synthesis of Bridged Macrocyclic Amino Alcohols as Compact Modules for Medicinal Chemistry. *Synth. Commun.* **2019**, *49*, 12−21.

(13) Watson, H. A., Jr.; O'Neill, B. T. A Reinvestigation and Improvement in the Synthesis of *meso*-2,5-Dibromoadipates by Application of Le Chatelier's Principle. *J. Org. Chem.* **1990**, *55*, 2950−2952.

(14) Given the biphasic conditions, adequate mixing is needed to obtain high selectivity and conversion, although the reaction does not appear to be highly sensitive to mixing effects.

(15) (a) Gotor-Fernandez, V.; Gotor, V. Enzymatic Aminolysis and Ammonolysis Processes in the Preparation of Chiral Nitrogenated Compounds. *Curr. Org. Chem.* **2006**, *10*, 1125−1143. (b) Lima, R. N.; dos Anjos, C. S.; Orozco, E. V. M.; Porto, A. L. M. Versatility of *Candida Antarctica* Lipase in the Amide Bond Formation Applied in Organic Synthesis and Biotechnological Processes. *Mol. Catal.* **2019**, *466*, 75−105.

(16) Starting ester **9** and the final amine **11** are both *meso* compounds and therefore achiral. Enzymatic amidation results in desymmetrization to give amide **10**, which is a chiral molecule. Since this chirality is inconsequential to the final product, we did not monitor the enantioselectivity of the enzymatic transformation.

(17) (a) De Zoete, M. C.; Kock-Van Dalen, A. C.; van Rantwijk, F.; Sheldon, R. A. A New Enzymatic Reaction: Enzyme Catalyzed Ammonolysis of Carboxylic Esters. *Biocatalysis* **1994**, *10*, 307−316. (b) Slotema, W. F.; Sandoval, G.; Guieysse, D.; Straathof, A. J. J.; Marty, A. Economically Pertinent Continuous Amide Formation by Direct Lipase-Cataltyzed Amidation with Ammonia. *Biotechnol. Bioeng.* **2003**, *82*, 664−669. (c) Gill, I.; Patel, R. Biocatalytic Ammonolysis of (5*S*)-4,5-dihydro-1*H*-pyrrole-1,5-dicarboxylic acid, 1-(1,1-dimethyl)-5-ethyl ester: Preparation of an Intermediate to the Dipeptidyl Peptidase IV Inhibitor Saxagliptin. *Bioorg. Med. Chem. Lett.* **2006**, *16*, 705−709.

(18) In the case of methanol, the higher reactivity of methyl esters resulted in formation of the corresponding bis-amide product, whereas the isopropyl ester was inert to the desired amidation reaction.

(19) Monitoring the reaction by GC shows the presence of both hexamethyldisiloxane (HMDSO) and ethoxytrimethylsilane (EtO-$SiMe_3$) in addition to HMDS added.

(20) For more details, see Basso, A.; Froment, L.; Hesseler, M.; Serban, S. *Eur. J. Lipid Sci. Technol.* **2013**, *115*, 468−472.

(21) (a) Gorman, L. A. S.; Dordick, J. S. Organic Solvents Strip Water off Enzymes. *Biotechnol. Bioeng.* **1992**, *39*, 392−397. (b) Yang, L.; Dordick, J. S.; Garde, S. Hydration of Enzyme in Nonaqueous Media is Consistent with Solvent Dependence of its Activity. *Biophys. J.* **2004**, *87*, 812−821. (c) Serdakowski, A. L.; Munir, I. Z.; Dordick, J. S. Dramatic Solvent and Hydration Effects on the Transition State of Soybean Peroxidase. *J. Am. Chem. Soc.* **2006**, *128*, 14272−14273. (d) Serdakowski, A. L.; Dordick, J. S. Enzyme Activation for Organic Solvents Made Easy. *Trends Biotechnol.* **2008**, *26*, 48−54.

(22) The addition of a comparable amount of EtOH to the reaction does not provide the same benefit as water.

(23) We have explored various strategies for trying to accurately quantify the amount of free vs bound water in the system, which we believe is important for further optimization; however, to date, this has been unsuccessful.

(24) The enzyme itself also contributes water to the system. The manufacturer specifies a water content of NMT of 5.0% (w/w).

(25) Enzyme recycling studies were performed on runs using significantly higher enzyme loadings (∼1 g/g) prior to identifying the beneficial impact of small amounts of water. When using the optimized conditions, we observed that the enzyme that had been subjected to the washing protocol showed decreased performance by ∼40−60% in subsequent runs; however, we did not attempt to further optimize the enzyme recycling for these conditions.

(26) Smith, S. C.; Bentley, P. D. Tandem Cyclisation and [2,3]-Stevens Rearrangement to 2-Substituted Pyrrolidines. *Tetrahedron Lett.* **2002**, *43*, 899−902.

(27) Like many amines, the freebase can discolor over time when exposed to oxygen; however, significant impurity growth is not observed with this discoloration.

(28) For recent reviews on cocrystals, see (a) Karimi-Jafari, M.; Padrela, L.; Walker, G. M.; Croker, D. M. Creating Cocrystals: A Review of Pharmaceutical Cocrystal Preparation Routes and Applications. *Cryst. Growth Des.* **2018**, *18*, 6370−6387. (b) Karagianni, A.; Malamatari, M.; Kachrimanis, K. Pharmaceutical Cocrystals: New Solid Phase Modification Approaches for the Formulation of APIs. *Pharmaceutics* **2018**, *10*, 18. (c) Childs, S. L.; Zaworotko, M. J. The Remergence of Cocrystals: The Crystal Clear Writing is on the Wall. *Cryst. Growth Des.* **2009**, *9*, 4208−4211.

(29) Abramov, Y. A.; Loschen, C.; Klamt, A. Rational Coformer or Solvent Selection for Pharmaceutical Cocrystallization or Desolvation. *J. Pharm. Sci.* **2012**, *101*, 3687−3697.

(30) Loschen, C.; Klamt, A. Solubility Prediction, Solvate and Cocrystal Screening and Tools for Rational Crystal Engineering. *J. Pharm. Pharmacol.* **2015**, *67*, 803−811.

(31) 4,4′-Dihydroxybiphenyl has been reported as a potential skin sensitizer and should be handled with appropriate safety precautions.

(32) (a) Asrar, J.; Toriumi, H.; Watanabe, J.; Krigbaum, W. R.; Ciferri, A.; Preston, J. Thermotropic Homopolyesters 1. The Preparation and Properties of Polymers Based on 4,4'dihydroxybiphenyl. *J. Polym. Sci., Part B: Polym. Phys.* **1983**, *21*, 1119−1131. (b) Krigbaum, W. R.; Watanabe, J.; Ishikawa, T. Thermotropic Polyesters 2. Investigation of the Mesophase Properties of Polymers Based on 4,4′-Dihydroxybiphenyl. *Macromolecules* **1983**, *16*, 1271−1279.

(33) 4,4′-Dihydroxybiphenyl is a key monomer used to synthesize polymers such as polyphenylsulfone (PPSU, PPSF, Radel) as well as an antioxidant used in the processing of rubber.

(34) See the Supporting Information for additional solubility data.

(35) We believe that this color is at least partially related to the ingoing quality of dibromide **1**; however, the exact factors controlling its appearance are not known.

(36) In some cases, small amounts of inorganic salts have been detected in the final material. In this case, a water reslurry can easily remove these, as the targeted cocrystal is essentially insoluble in water.

https://doi.org/10.1021/acs.oprd.1c00120
Org. Process Res. Dev. 2021, 25, 1419−1430